A Five-port Integrated Planar Ultra Wideband and Narrowband Antennas System Using Excitation Switching Reconfigurable Technique for Cognitive Radio Applications

Abdulaziz Dessalew Tadesse
Kalinga Institute of Industrial Technology
OM PRAKASH ACHARYA (omprakash.acharyafet@kiit.ac.in)
Kalinga Institute of Industrial Technology https://orcid.org/0000-0002-3858-7711
Sudhakar Sahu
Kalinga Institute of Industrial Technology

Research Article

Keywords: Cognitive radio,Integrated UWB/NB antennas,MIMO, Sub 6GHz 5G, UWB

Posted Date: July 19th, 2022

DOI: https://doi.org/10.21203/rs.3.rs-1811273/v1

Version of Record: A version of this preprint was published at Wireless Personal Communications on April 24th, 2023. See the published version at https://doi.org/10.1007/s11277-023-10443-y.

Abstract

This work presents an integrated planar five-element antennas system for cognitive radio (CR) applications. The proposed system is composed a ultra-wideband (UWB) antenna for sensing the radio spectrum and four different narrowband (NB) antennas for conducting the communication tasks. The overall antenna system is printed on FR-4 substrate of 50 mm × 50 mm × 1.6 mm dimension. The UWB antenna-coupled at port 5 (P5) is designed for sensing the 3.1 GHz to 10.6 GHz un-licensed UWB band. The first NB antenna attached to port 1(P1) covers 5 GHz to 11.4 GHz wideband frequency, whereas the paired NB antennas located at port 2 and port 3 (P2 & P3) consists of two similar antennas to achieve MIMO operation and provides 3.05 GHz to 3.75 GHz and 4.9 GHz to 6.1 GHz dual-band operation.The last NB antenna accessible at port 4 (P4) operates in dual-band frequencies of 3.7 GHz to 4.92 GHz and 8.3 GHz to 11.3 GHz. These attained resonant bands cover applications, notably Wi-MAX 3.5 GHz, Upper WLAN, sub 6 GHz 5G, and X-bands in the full UWB spectrum.The minimum isolation among all UWB and NB antennas is 16 dB over the working bands. The MIMO performances of the port 2 and port 3 antenna pairs have been computed considering the envelope correlation coefficient and mean effective gain, and found within their practical limits. The measured results are validated and show a good matching with the simulated ones.The low profile and planar features of the suggested antenna make it a possible choice to be assimilated within small wireless devices applicable in CR communication.

1 Introduction

In present-day communication system, the development of diverse wireless technologies results in enormous bandwidth requirements. However, the frequency spectrum is a scarce resource that cannot be infinitely allocated because of financial and physical constraints. The shortage is mostly due to inefficient regulation on spectrum utilization where the licenced spectrum channels are often in idle condition [1]. Thus, there must be some ways to resolve the spectrum scarcity and wastage problems. In 2002, FCC introduced ways such as spectrum leasing, spectrum reallocation, and spectrum sharing [2–4]to address the problems.

To improve spectrum utilization efficiency with the use of vacant channels across broad frequency ranges, CR is the most favourable technology[5, 6]. In particular, a CR system is sensitive enough to detect the spectrum utilization and assign services to the vacant section of the spectrum without interfering with other users. To accomplish these tasks, a UWB antenna to sense the unused spectrum and reconfigurable NB antenna to do the communication jobs are required in the antenna design procedure [7, 8].

Because of the advancement in printed antenna technology, several antennas [9–16]for UWB communication have been explored to achieve wideband characteristics. Different types of printed CR antennas applying frequency reconfiguration methods such as optical switching[17],[18], diodes [19–22], material changes and mechanical rotation [23] have been proposed over the previous few years. However, these reconfigurable mechanisms have their unavoidable limitations like non-linear effects of switches, slow tuning operation, mutual coupling caused by the biasing lines, consumption of high power, external complex biasing circuitries, and fabrication complexity [24]. Additionally, the practical implementation of these reconfigurable schemes is challenging.

Since then, there have been numerous dual-port integrated antennas developed with wideband and NB operation for CR applications[25–31]. However, due to the NB characteristics of the single antenna, it is impossible to entirely cover the whole UWB band (3.1 GHz to 10.6 GHz). To cover the whole spectrum and overcome problems associated with reconfiguration techniques, multiple NB antennas integrated with the UWB antenna have been attempted [32–35]. However, the integration of UWB and multiple NB antennas inside the same volume and on a limited space is a challenging problem for antenna designers as the resulted antenna coupling degrades its performances. To enhance the port isolation of the above-mentioned integrated UWB and NB antennas, separate ground plane technique has been applied, which is not desirable in practical designs. Therefore, the design should take the compactness of the antenna and the subsequent isolation issues into account.

At the same time, the high data rate services and improved channel capacity demands of modern technologies including 5G drive the CR system to incorporate MIMO antennas at its wireless ends [36]. Thus far, researches integrating MIMO antennas with CR system have been done in [37–44]. This research is primarily aimed at increasing the efficiency of spectrum utilization by offering numerous communication jobs at a time when the UWB sensing antenna detects several unused spectrum holes, which cannot be possible with conventional single or dual-port antennas. The integrated NB antennas can encompass the entire UWB band. Also, the suggested antenna retains an acceptable isolation level between the sensing and communication antennas even with an interconnected ground plane without external complex decoupling structure. The antennas at P2, P3, and P4 are meandered [45]to make them compact and increase the physical separation between neighbouring antennas.

This article presents a planar five-port integrated slotted circular-shaped UWB antenna and NB antennas for possible application in CR environment. The basis for the presented antenna is the CR antenna recommended in [34], which incorporates multiple NB antennas and excitation switching reconfigurable technique.In this switching technique, the NB antenna whose working frequency corresponds to the identified spectrum hole will be selected to provide the required communication task. The suggested antenna can overcome the limitations present in conventional reconfigurable methods. Among the four NB antennas, the similar pair of antennas located at P2 and P3 are meant for MIMO operation in the lower sub 6GHz 5G and the upper WLAN bands.

Thefollowing is the structure of the paper. Section 2 provides a detailed explanation regarding the design procedures of the UWB and the single/dual-band NB antennas. Section 3 discusses the results obtained under each operative condition. The MIMO performance parameters are presented in Sect. 4, whereas Sect. 5 brings the work to a close.

2 Antenna Geometry And Design

The proposed five port MIMO antenna is built on an FR4-epoxy substrate material having a relative permittivity of 4.4, loss tangent of 0.02, and size of 50 mm × 50 mm ×1.6mm. The structural design and optimization of antenna dimensions are performed using HFSS ver. 21 3D-simulator. To obtain a wide impedance bandwidth at the chosen frequencies, the antenna elements are supported by a partial ground plane. The schematic and design parametric values are depicted in Fig. 1 and Table 1.Comprehensive explanations of the UWB antenna, single/dual-band antennas, and the two-port MIMO antennas are provided in this section.

Table 1
Design parametric values of the proposed five-port antenna

Parameters	L	W	ag	Lg	e	k	cw	dw	ew	cx	Lf
Value (mm)	50	50	3	8	5.5	0.5	12	6	15	2	8.7
Parameters	wf	ay	R	h1	L1	L2	L3	L4	L5	L6	L7
Value (mm)	2.5	10	7.5	4	12.2	3	6	4.3	6	3	8
Parameters	L8	L9	W2	W3	W4	W5	W6	W7	W8	W9	
Value (mm)	9.5	4	8	5.2	4	5.2	2.75	6	3.3	6	

2.1 The UWB Antenna Design Procedure

The UWB antenna placed at port 5 (P5) has passed through three evolutionary design steps. In step 1, a circular monopole is printed on a partial ground plane backed substrate material. This basis for design is the equation given in [46]. The resulting antenna, designated as Ant_1, achieves an operating frequency starting from 3.5 GHz. In step 2, the conventional ground slot technique is applied beneath the feed line for impedance matching enhancement. At this stage of Ant_2, a 3.5 GHz to 10.6 GHz impedance bandwidth is obtained. However, the above two design stages couldn't attain the lower 3.1 GHz UWB band. To include this frequency range, a slot is removed from the main patch in step 3. The slot enables to have extra current path on the patch and lowers the resonance frequency to 2.6 GHz. This UWB sensing antenna, Ant_3, covers the whole 3.1 GHz to 10.6 GHz spectrum with a better impedance matching. This last step design is therefore established as the basic UWB antenna. The proposed UWB antenna geometry and its reflection coefficient results for each design stage are depicted in Fig. 2.

2.2 The Single/Dual-band Communicating Antennas Design Procedure

After completing the UWB antenna design, the remaining single/dual-band antennas intended for communication purposes are incorporated on the same substrate as shown in Fig. 1a. In these designs, maximum attention is given to make them compact, which contributes to maximizing the port isolation between them and the UWB antenna while working in their respective operating conditions. The antennas linked at ports P1, P2, P3, P4, and P5 are designated as Ant (P1), Ant (P2), Ant (P3), Ant (P4), and Ant (P5), respectively, in the subsequent discussions.

Ant (P1)

The antenna available at port 1 (P1) comprises of a dual-arm monopole supported by a partial ground plane at its back targeting a wide bandwidth,as can be seen in Fig. 4a. The resonance effects of the long and short arms of the antenna contribute to this wide impedance bandwidth.

Ant (P2) and Ant (P2)

The antenna geometries and their dimensions for P2 & P3 are shown in Fig. 1a. These two antennas are identical in geometry and constructed from the unbalanced arm, modified Y-shaped monopoles. To make the radiating structure compact, a meander line concept is applied [47]. The main target is to design a two-port dual-band MIMO antenna resonating at the lower sub 6 GHz 5G frequency (3.3 GHz to 3.6 GHz) band and also include the WLAN upper-frequency band. A two-T-shaped stub is incorporated into the ground plane to decrease mutual coupling between the two meander line antennas. Theisolation impact of the ground stub is analysed using transmission coefficient and surface current distribution plots.

Ant (P4)

The antenna geometry accessible at P4 is shown in Fig. 1a. Its feed line is located at the other edge of the substrate to increase the port isolation from the UWB antenna. The main objective is to design a monopole antenna covering the frequencies around 4 GHz, which are not covered by Ant (1), Ant (2), and Ant (3).

The UWB antenna located at P5 is employed as a spectrum sensor and the remaining antennas, which are placed at the other four ports (P1, P2, P3& P4), serve the communication task. When a void in the spectrum is detected by the UWB antenna, the associated NB antenna is picked for communication using excitation reconfigurable switching technique.The other antennas stay idle. Due to the presence of 5 port radiators, there are possibly three cases of operation when a spectrum is detected. These cases are the UWB sensing antenna and Ant (P1), the UWB antenna and the two-element MIMO generated by Ant (P2) and Ant (P3), and the UWB antenna and Ant (P4). Figure 1a depicts the dimensions of the four NB antennas accompanied by the UWB antenna. In this paper, the discussion of results is provided in these three operative conditions as will be examined in the next section.

3 Results And Discussion

Specifically, in the below sub-sections, the simulated and measured scattering parameters, surface current distributions, radiation patterns, gains, and radiation efficiencies of the UWB and NB antennas are studied under each operation case. A matching load of 50 Ω is used to terminate the antennas in the idle state during the simulation and measurement processes.

3.1 Operative Condition 1

When the UWB antenna senses the spectrum hole in this case, Ant (P1) starts its communication task whereas the remaining antennas are terminated with 50 Ω loads. For the sensing task, the UWB antenna is required to maintain stable radiation patterns throughout its scanning frequency range [36]. For confirmation purpose, its radiation patterns at all communication antenna resonant frequencies (3.4 GHz, 4 GHz, 5.6 GHz, 6 GHz, and 10 GHz) and its peak gain are depicted in Fig. 3. As presented in Fig. 3a-e, the UWB sensing antenna has almost consistent dipole type and omnidirectional radiation patterns in E-plane (XZ-plane) and H-plane (YZ-plane), respectively. Figure 3f shows the UWB antenna peak gains through its working frequency range.

Thesimulated and measured reflection and transmission coefficients (S11, S55, and S51) of the UWB antenna and Ant (P1) are shown in Fig. 4. As illustrated in Fig. 4a, the UWB antenna has 2.1 GHz to 11.8 GHz measured working frequency range, which embraces the whole UWB band (3.1 GHz to 10.6 GHz). Besides, Ant (P1) yields 5.7GHz to 11.6 GHz simulated and 5 GHz to 11.4 GHz measured impedance bandwidth. Figure 4b displays the simulated and measured transmission coefficient plot and,from the graph, it is observed that an isolation value greater than 16 dB is obtained in the operating band. Figure 5a shows Ant (P1) simulated and measured radiation patterns in the E and Y orthogonal planes at 6 GHz, whereas Fig. 5b displays the measurementsetup.

3.2 Operative Condition 2

In this instance, the UWB antenna does the spectrum scanning task, whereas Ant (P2) and Ant (P3) are employed for communication purposes. At this time, Ant (P1) and Ant (P4) remain idle. As stated, these communication antennas are intended to coverthe lower sub 6GHz 5G band and the upper WLAN band. The simulated and measured reflection and transmission coefficients (S22, S33, S55, S32, S52, and S53) of the UWB antenna and Ant (P2) and Ant (P3) are shown in Fig. 6. The UWB antenna attains a 3.05 GHz to 12 GHz measured frequency which includesthe complete UWB band as depicted in Fig. 6a.Also, the port isolation between it and Ant (P2) is more than 16 dB. Figure 6b shows the dual-band resonance of Ant (P2) along with the port isolation in between the Ant (P3). As shown in the figure, the antenna attains closely matched simulated and measured impedance bandwidths of 3.05 GHz to 3.75 GHz and 4.9 GHz to 6.1 GHz with 16 dB minimum port isolation at both operation bands.

To confirm the isolation performance of the applied decoupling structure, the transmission coefficient S32 is plotted in Fig. 7 without and with single and two T-stubs. As illustrated in the figure,theapplication of ground plane stub results in mutual coupling reduction at both bands.

To additionally clarify the significance of the ground stub to reduce the mutual coupling, surface current distribution without and with T-shaped stub at 5.6 GHz is shown in Fig. 8 by exciting P2 and terminating P3. As displayed in Fig. 8b, the induced current from the excited antenna is distributed to the stub. Thus, the creation of an additional current path due to the presence of the stub weakens the current reaching at the second antenna, which leads to an isolation improvement between the antennas.

3.3 Operative Condition 3

In this condition, the UWB antenna works to detect unused spectrum holes and Ant (P4) is responsible for the communication task. Ant (P1), Ant (P2), and Ant (P3) remain idle. This communication antenna is aimed to function at the remaining frequency ranges of the UWB band left uncovered by the other NB antennas, Ant (P1), Ant (P2), and Ant (P3). The simulated and measured S44, S55, and S54 parameters of the UWB antenna and Ant (P4) are shown in Fig. 9. The UWB antenna has simulated and measured ranges of 3 GHz to 11.7 GHz and 2.3 GHz to 11.3 GHz, respectively, which include the 3.1 GHz to 10.6 GHz UWB band as shown in Fig. 9a. Figure 9b shows the dual-band resonance of the NB antenna along with the port isolation in between it and the UWB antenna. The figure shows that the antenna attains closely matched simulated and measured wide impedance bandwidths of 3.7 GHz to 4.92 GHz and 8.3 GHz to 11.3 GHz.Moreover, the measured port isolation between it and the UWB antenna is greater than 16 dB. Figure 10 shows simulated and measured 2-D radiation patterns of Ant (P4) at 4 GHz and 10 GHz. Table 2 shows the measured impedance bandwidths of the UWB and the single/dual-band communication antennas at corresponding operative conditions.

Table 2
Status of antennas at respective operative conditions

Antenna	Condition 1	Condition 2	Condition 3
UWB	2.1 GHz to 11.8 GHz	3.05 GHz to 12 GHz	2.3 GHz to 11.3 GHz
Ant (P1)	5 GHz to 11.4 GHz	OFF	OFF
Ant (P2) & Ant (P3)	OFF	3.05 GHz to 3.75 GHz 4.9 GHz to 6.1 GHz	OFF
Ant (P4)	OFF	OFF	3.7 GHz to 4.92 GHz 8.3 GHz to11.3 GHz

The simulated and measured gains of the NB antennas mentioned under each operative condition are shown in Fig. 11. As shown in Fig. 11a, the gain of Ant (P1) varies from 3.25 dB to 7.2 dB while the gain of Ant (P4) varies from 5.12 dB to 6.53 dB in its first working band and from 5.70 dB to 7.75 dB in its second operating band. The gain plot presented in Fig. 11b shows that the MIMO antenna composed of Ant (P2) and Ant (P3) has 5.12 dB to 6.32 dB and 5.02 dB to 5.93 dB peak gains at the chosen ranges. The proposed antenna fabricated model is given in Fig. 12.

4 Mimo Performance Analysis

Significant parameterssuch as envelope correlation coefficient (ECC), diversity gain (DG), and mean effective gain (MEG) are investigated in this section in order to assess the diversity performance of the two-element MIMO antenna.

4.1 ECC and DG

The ECC is a significant metric that reflects the extent of isolation or correlation between wireless communication channels. Mathematically, it can be computed from S-parameters or far-field antenna radiation patterns using Eq. 1 and Eq. 2, respectively, with an acceptable maximum value of 0.5 to obtain the required diversity performance [1].

$$ECC = \frac{\left|{S^*}_{11}S_{12} + {S^*}_{21}S_{22}\right|^2}{\left(1 - \left|S_{11}\right|^2 - \left|S_{21}\right|^2\right)\left(1 - \left|S_{22}\right|^2 - \left|S_{12}\right|^2\right)}$$

1

$$ECC = \frac{\left|\iint_{4\pi} \left[F_i\left(\theta,\phi\right) * F_j\left(\theta,\phi\right)\right] d\Omega\right|^2}{\iint_{4\pi} \left|F_i\left(\theta,\phi\right)\right|^2 d\Omega \iint_{4\pi} \left|F_j\left(\theta,\phi\right)\right|^2 d\Omega}$$

2

where$F_i\left(\theta,\phi\right)$and $F_j\left(\theta,\phi\right)$symbolizes far-field radiation patterns.

Likewise, DG is an additionalparameter to measure the improvement in signal-to-noise ratio as a result of a diversity scheme which can be computed from the resulted ECC values [48] as given in Eq. 3.

$$DG = 10\sqrt{1 - \left(ECC\right)^2}$$

3

Figure 13a shows the dual-band MIMO antennaECC and DG simulated and measured results. As can be seen, ECC less than 0.02 and DG nearly 10 dB are obtained for both operation bands suggesting that the proposed antenna is appropriate for applications in a multipath fading channel.

4.2 MEG

MEG is the parameter that defines the ratio of average powers of the diversity antenna and the isotropic antenna. The difference of MEGs of the two ports (MEG1-MEG2) should be within ± 3 dB for achieving enhanced diversity performance[49].Mathematically, it is expressed by Eq. 4 and Eq. 5.

$$MEG1 = 0.5\eta_{1,rad} = 0.5\left[1 - \left|S_{11}\right|^2 - \left|S_{12}\right|^2\right]$$

4

$$MEG2 = 0.5\eta_{2,rad} = 0.5\left[1 - \left|S_{12}\right|^2 - \left|S_{22}\right|^2\right]$$

5

where$\eta_{1,rad}$and $\eta_{2,rad}$represent radiation efficiencies associated with port 1 and port 2. The deviation MEG12 = MEG1-MEG2 is bounded to 3 dB as expressed in Eq. 6.

$$\left|MEG1 - MEG2\right| < 3dB$$

6

The simulated and measured MEG deviations shown in Fig. 13b range from − 0.55 dB to 1.77 dB in both working bands satisfy the necessary MEG level.

The comparison of the proposed antenna in relation to other CR antennas is given in Table 3. In accordance with the information given in the table, thissuggested five-port integrated UWB/NB antenna covers the full UWB band from 3.1GHz to 10.6 GHz. In addition, the antenna is printed on a compact size substrate with a shared ground plane, providing high port isolation and MIMO performances without the requirement of a complex decoupling structure. The obtained resonant bands encompass diverse applications such as Wi-MAX 3.5 GHz, Upper WLAN, sub 6 GHz 5G, and X-bands in the complete UWB band. Thus, this antenna can be a possible alternative to be assimilated within small wireless devices applicable in CR communication.

Table 3
Comparison of the proposed antenna with other integrated and CR MIMO antennas

Ref.	**Dimension (mm^2)**	**# Ant.**	**UWB range (GHz)**	**NB frequencies**	**I_{min} (dB)**	**Reconfigurable technique**	**MIMO operation/ECC**
[25]	77 × 58.8	2	2.6–11	4.9–6.2	10	Not applied	No
[26]	68 × 54	2	3–11	4.9-5.35and very narrow resonances at 4, 8 and 10 GHz	18	external tuning circuits	No
[27]	75.7 × 58.35	2	2.1–12	4.4–5.4, 6.4–7.6	10	Not applied	No
[28]	63.6 × 37	2	2–12	5.7–5.9	20	Not applied	No
[30]	58 × 65.5	2	3.3–11	3.4–4.85, 5.3–9.15	10	rotational motion	No
[32]	30 × 30	3	2.76–13.9	6.36–6.63, 8.78–9.23, 7.33–7.7, 9.23–9.82	20	Excitation switching	No
[34]	40 × 36	5	3.1–10.6	Five bands from 3.1–10 .6 GHz	16	Excitation switching	No
[35]	42 × 50	4	3.1–10.6	2.9–5.38, 5.31–8.62, 8.48–11.02	17.3	Excitation switching	No
[36]	100 × 120	4	2.3–5.5	2.5–4.2	15	Varactor and PIN diodes	Yes/0.02
[39]	60 × 120	8	Not given	1.6–2.48	11	varactor diodes	Yes/0.09
[40]	60 × 120	4	Not given	1.8–2.45	10	varactor diodes	Yes/0.186
[41]	80 × 80	2	2.35–5.9	2.6–3.6	15	varactor diodes	Yes/0.06

Key: # Ant. = Number of antennas including the UWB and NB antennas, I_{min} = minimum port isolation.

Ref.	Dimension (mm^2)	# Ant.	UWB range (GHz)	NB frequencies	I_{min} (dB)	Reconfigurable technique	MIMO operation/ECC
[42]	60 × 120	2	1-4.5	0.9–2.6	12.5	Varactor and PIN diodes	Yes/0.19
[43]	60 × 120	4	0.75–7.65	1.77–2.51	10	varactor diodes	Yes/0.248
[44]	100 × 50	2	Not given	1.42–2.27	12	varactor diodes	Yes/0.2
This work	**50 × 50**	**5**	**3.05–11.3**	**3.05–3.75**, **3.7–4.92**, **4.9–6.1**, **5–11**, **8.3–11.3**,	**16**	**Excitation switching**	**Yes/0.02**
Key: # Ant. = Number of antennas including the UWB and NB antennas, I_{min} = minimum port isolation.							

5 Conclusion

This paper presents a five-port UWB and NB antennas system using excitation switching reconfigurable technique for CR applications. The UWB antenna has a minimum of 3.05 GHz to 11.3 GHz impedance bandwidth to span the complete 3.1 GHz to 10.6 GHz UWB spectrum under all three operative conditions. The first antenna linked at P1 yields a single band (5 GHz to 11.4 GHz), the dual-port MIMO antenna allied at P2 and P3 achieves a dual-band (3.05 GHz to 3.75 GHz and 4.9 GHz to 6.1 GHz), and the antenna connected at P4 results in dual-band (3.7 GHz to 4.92 GHz and 8.3 GHz to 11.3 GHz) to completely cover the UWB spectrum. The proposed system can simultaneously execute three communication tasks to improve the efficiency of spectrum utilization, which is the fundamental motive behind CR technology. The port isolation between antennas mentioned in each operative condition was below 16 dB, which is adequate for an antenna system integrated on an interconnected ground plane. The MIMO antenna linked at P2 and P3 has ECC, DG, and MEG diversity performances within acceptable ranges. Its planar nature, simplicity, compact size, and better performances make the proposed antenna system a good candidate for CR environment spectrum sensing and communication.

Declarations

Funding

“The authors declare that no funds, grants, or other support were received during the preparation of this manuscript.”

Competing Interests

“The authors have no relevant financial or non-financial interests to disclose.”

Data Availability

Data sharing not applicable to this article as no datasets were generated or analysed during the current study.

Author Contribution:

All authors contributed to the study conception and design. The implementation part was carried by Abdulaziz Dessalew Tadesse (ADT). The first draft of the manuscript was written by ADT. Om Prakash Acharya revised the manuscript. All authors have read and approved the final manuscript.

References

1. Pahadsingh, S., & Sahu, S. (2018). Four port MIMO integrated antenna system with DRA for cognitive radio platforms. *AEU-International Journal of Electronics and Communications*, *92*, 98–110.
2. Al-husseini, M., Kabalan, K. Y., El-hajj, A., & Christodoulou, C. G. (2010). Cognitive Radio: UWB Integration and Related Antenna Design. *New trends in technologies: control, management, computational intelligence and network systems*(pp. 213–215).
3. Tawk, Y., Bkassiny, M., El-Howayek, G., Jayaweera, S.K., Avery, K., & Christodoulou, C. G. (2011). Reconfigurable front-end antennas for cognitive radio applications. *IET Microwaves, Antennas & Propagation*, *5*(8), 985–992.
4. Jayaweera, S. K., & Mosquera, C. (2009). A Dynamic Spectrum Leasing (DSL) Framework for Spectrum Sharing in Cognitive Radio Networks. Proceedings of the IEEE Forty- Third Asilomar Conference on Signals, Systems and Computers, Pacific Grove, California, 1819–1823.
5. Mitola, J., & Maguire, G. Q. (1999). Cognitive Radio: Making Software Radios More Personal. *IEEE Personal Communications*, *6*(4), 13–18.
6. Haykin, S. (2005). Cognitive radio: brain-empowered wireless communications. *IEEE Journal on Selected Areas in Communications*, *23*(2), 201–220.
7. Hall, P. Gardner, S., & Faraone, A. (2012). Antenna Requirements for Software Defined and Cognitive Radios. *Proceedings of the IEEE*, *100*(7), 2262–2270.
8. Safatly, L., Bkassiny, M., Al-husseini, M., & El-hajj, A. (2014). Cognitive Radio Transceivers: RF , Spectrum Sensing , and Learning Algorithms Review. *International Journal of Antennas and Propagation*, *2014*.
9. Ojaroudi, M., & Ojaroudi, N. (2014). Ultra-wideband small rectangular slot antenna with variable band-stop function. *IEEE Transactions on Antennas and Propagation*, *62*(1), 490–494.

10. Shafique, K., Khawaja, B. A., Tarar, M. A., Khan, B. M., Mustaqim, M., & Raza, A. (2016). A wearable ultra-wideband antenna for wireless body area networks. *Microwave and Optical Technology Letters*, *58*(7), 1710–1715.
11. Peng, L., Wen, B. J., Li, X. F., Jiang, X., & Li, S. M. (2016). CPW Fed UWB Antenna by EBGs with Wide Rectangular Notched-Band. *IEEE Access*, *4*, 9545–9552.
12. Singh, T., Ali, K. A., Chaudhary, H., Phalswal, D. R., Gahlaut, V., & Singh, P. K. (2018). Design and analysis of reconfigurable microstrip antenna for cognitive radio applications. *Wireless Personal Communications*, *98*(2), 2163–2185.
13. Malekpoor, H., & Hamidkhani, M. (2019). Compact multi-band stacked circular patch antenna for wideband applications with enhanced gain. *Electromagnetics*, *39*(4), 241–253.
14. Lakrit, S., Das, S., El Alami, A., Barad, D., & Mohapatra, S. (2019). A compact UWB monopole patch antenna with reconfigurable Band-notched characteristics for Wi-MAX and WLAN applications. *AEU - International Journal of Electronics and Communications*, *105*, 106–115.
15. Lakrit, S., Das, S., Ghosh, S., & Madhav, B. T. P. (2020). Compact UWB flexible elliptical CPW-fed antenna with triple notch bands for wireless communications. *International Journal of RF and Microwave Computer-Aided Engineering*, *30*(7), 1–14.
16. Elmobarak, H. A., Abdul Rahim, S. K., Castel, X., & Himdi, M. (2019). Flexible conductive fabric E-glass fibre composite ultra-wideband antenna for future wireless networks. *IET Microwaves, Antennas & Propagation*, *13*(4), 455–459.
17. Tawk, Y., Costantine, J., Hemmady, S., Balakrishnan, G., Avery, K., & Christodoulou, C. G. (2012). Demonstration of a cognitive radio front end using an optically pumped reconfigurable antenna system (OPRAS). *IEEE Transactions on Antennas and Propagation*, *60*(2), 1075–1083.
18. Ali, A., Topalli, K., Ramzan, M., Alibakhshikenari, M., Khan, T. M., Altintas, A., & Colantonio, P. (2019). Optically reconfigurable planar monopole antenna for cognitive radio application. *Microwave and Optical Technology Letters*, *61*(4), 1110–1115.
19. Cai, Y., Guo, Y. J., & Bird, T. S. (2012). A frequency reconfigurable printed yagi-uda dipole antenna for cognitive radio applications. *IEEE Transactions on Antennas and Propagation*, *60*(6), 2905–2912.
20. Augustin, G., Chacko, B. P., & Denidni, T. A. (2014). Electronically reconfigurable uni-planar antenna for cognitive radio applications. *IET Microwaves, Antennas and Propagation*, *8*(5), 367–376.
21. Kingsly, S., Thangarasu, D., Kanagasabai, M., Alsath, M. G. N., Thipparaju, R. R., Palaniswamy, S. K., & Sambandam, P. (2018). Multiband reconfigurable filtering monopole antenna for cognitive radio applications. *IEEE Antennas and Wireless Propagation Letters*, *17*(8), 1416–1420.
22. Chatterjee, J., Mohan, A., & Dixit, V. (2020). Frequency reconfigurable slot antenna using metasurface for cognitive radio applications. *IET Microwaves, Antennas and Propagation*, *14*(3), 194–202.
23. Tsolis, A., Michalopoulou, A., & Alexandridis, A. A. (2020). Use of conductive zip and Velcro as a polarisation reconfiguration means of a textile patch antenna. *IET Microwaves, Antennas and Propagation*, *14*(7), 684–693.

24. Nella, A., & Gandhi, A. S. (2017). A Survey on Planar Antenna Designs for Cognitive Radio Applications. *Wireless Personal Communications*, *98*(1), 541–569.
25. Augustin, G., & Denidni, T. A. (2012). An Integrated Ultra Wideband / Narrow Band Antenna in Uniplanar Configuration for Cognitive Radio Systems. *IEEE Transactions on Antennas and Propagation*, *60*(11), 5479–5484.
26. Ebrahimi, E., Member, S., Kelly, J. R., & Hall, P. S. (2011). Integrated Wide-Narrowband Antenna for Multi-Standard Radio. *IEEE Transactions on Antennas and Propagation*, *59*(7), 2628–2635.
27. Pahadsingh, S., & Sahu, S. (2016). A two port UWB-dual narrowband antenna for cognitive radios. *Microwave and Optical Technology Letters*, *58*(8), 1973–1978.
28. Sahnoun, N., & Messaoudene, I. (2015). Integrated Flexible UWB / NB Antenna Conformed on a Cylindrical Surface. *Progress in Electromagnetics Research Letters*, *55*, 121–128.
29. Nachouane, H., Najid, A., Tribak, A., & Riouch, F. (2016). Dual Port Antenna Combining Sensing and Communication Tasks for Cognitive Radio. *International Journal of Electronics and Telecommunications*, *62*(2), 121–127.
30. Tawk, Y, & Christodoulou, C. G. (2009). A New Reconfigurable Antenna Design for Cognitive Radio. *IEEE Antennas and Wireless Propagation Letters*, *8*, 1378–1381.
31. Kantemur, A., Tak, J., Siyari, P., Abdelrahman, A. H., Krunz, M., & Xin, H. (2020). A Novel Compact Reconfigurable Broadband Antenna for Cognitive Radio Applications. *IEEE Transactions on Antennas and Propagation*, *68*(9), 6538–6547.
32. Kumar, N. A., & Gandhi, A. S. (2016). A Compact Novel Three-Port Integrated Wide and Narrow Band Antennas System for Cognitive Radio Applications. *International Journal of Antennas and Propagation*, *2016*.
33. Pahadsingh, S., & Sahu, S. (2017). Planar UWB integrated with multi narrowband cylindrical dielectric resonator antenna for cognitive radio application. *AEU - International Journal of Electronics and Communications*, *74*, 150–157.
34. Nella, A., Member, S., & Gandhi, A. S. (2018). A Five-Port Integrated UWB and Narrowband Antennas System Design for CR Applications. *IEEE Transactions on Antennas and Propagation*, *66*(4), 1669–1676.
35. Yeonjeong, O., & Jin, Y. (2019). A Compact Four-Port Coplanar Antenna Based on an Excitation Switching Reconfigurable Mechanism for Cognitive Radio Applications. *Applied Sciences*, *9*(15).
36. Thummaluru, S. R., , Ameen, M., & Chaudhary, R. K. (2019). Four-Port MIMO Cognitive Radio System for Midband 5G Applications. *IEEE Transactions on Antennas and Propagation*, *67*(8), 5634–5645.
37. Tawk, Y., Costantine, J., & Christodoulou, C. G. (2014). Reconfigurable Filtennas and MIMO in Cognitive Radio Applications. *IEEE Transactions on Antennas and Propagation*, *62*(3), 1074–1083.
38. Hussain, R., & Sharawi, M. S. (2015). A cognitive radio reconfigurable MIMO and sensing antenna system. *IEEE Antennas and Wireless Propagation Letters*, *14*, 257–260.

39. Riaz, S., & Zhao, X. (2018). An 8-Element Frequency-Agile MIMO Communication Antenna System for CR Front-End Applications. *Progress In Electromagnetics Research C*, *84*, 75–85.
40. Hussain, R., Ghalib, A., & Sharawi, M. S. (2017). Annular slot-based miniaturized frequency-agile MIMO antenna system. *IEEE Antennas and Wireless Propagation Letters*, *16*, 2489–2492.
41. Alam, T., Thummaluru, S. R., & Chaudhary, R. K. (2018). Two-Port MIMO Wide-Band Antenna With Two-Port MIMO Reconfigurable Antenna for cognitive radio platforms. *2018 IEEE Indian Conference on Antennas and Propogation (InCAP)*, 1–4.
42. Zhao, X., Riaz, S., & Geng, S. (2019). A Reconfigurable MIMO / UWB MIMO Antenna for Cognitive Radio Applications. *IEEE Access*, *7*, 46739–46747.
43. Hussain, R., Sharawi, M. S., & Shamim, A. (2018). An Integrated Four-Element Slot-Based MIMO and a UWB Sensing Antenna System for CR Platforms. *IEEE Transactions on Antennas and Propagation*, *66*(2), 978–983.
44. Riaz, S., Zhao, X., & Geng, S. (2020). A frequency reconfigurable MIMO antenna with agile feedline for cognitive radio applications. *International Journal of RF and Microwave Computer-Aided Engineering*, *30*(3).
45. Raza, A., Khan, M. U., Tahir, F. A., Hussain, R., & Sharawi, M. S. (2018). A 2-element meandered-line slot-based frequency reconfigurable MIMO antenna system. *Microwave and Optical Technology Letters*, *60*(11), 2794–2801.
46. Balanis, C. A. (2005). Microstrip Antennas. In *Antenna Theory: Analysis and Design* (3rd edn., pp. 769–830). John Wiley & Sons.
47. Chouhan, S.,Panda, D.K., Gupta, M., Singhal, S. (2017). Meander line MIMO antenna for 5.8 GHz WLAN application. *International Journal of RF and Microwave Computer-Aided Engineering*, *28*(4).
48. Srikar, D., & Anuradha, S. (2019). Twelve port MIMO antenna with polarisation diversity for cognitive radio applications. *Electronics Letters*, *55*(22), 2019–2021.
49. Kazim, R., & Owais, O. (2017). Dual-band MIMO dielectric resonator antenna for WiMAX / WLAN applications. *IET Microwaves, Antennas & Propagation*, *11*(1), 113–120.

Figures

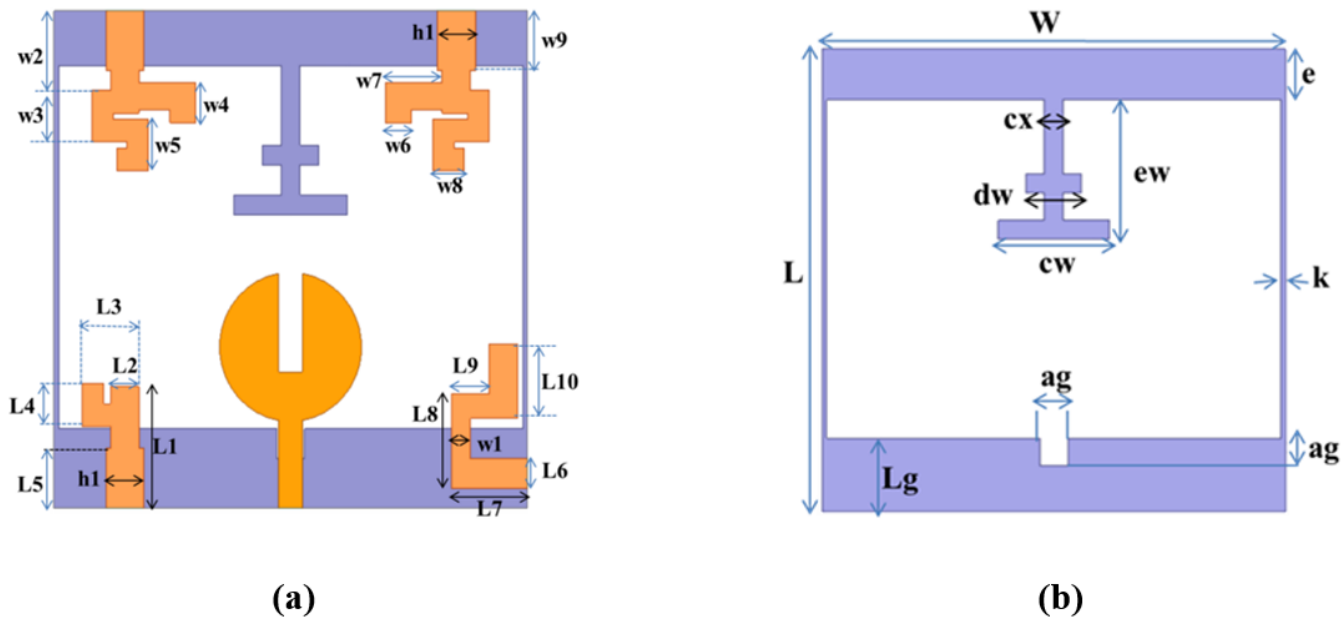

Figure 1

The five-port antenna **a** Top view,**b** Bottom view

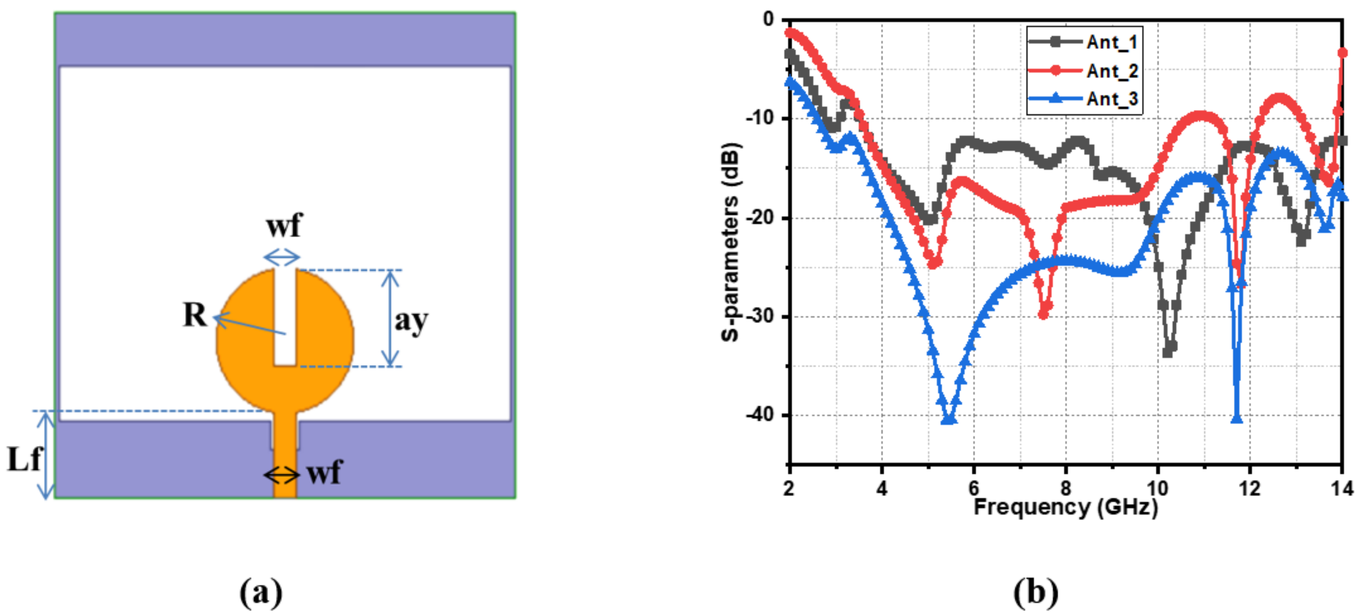

Figure 2

The UWB antenna**a** Geometry, **b** Reflection coefficient

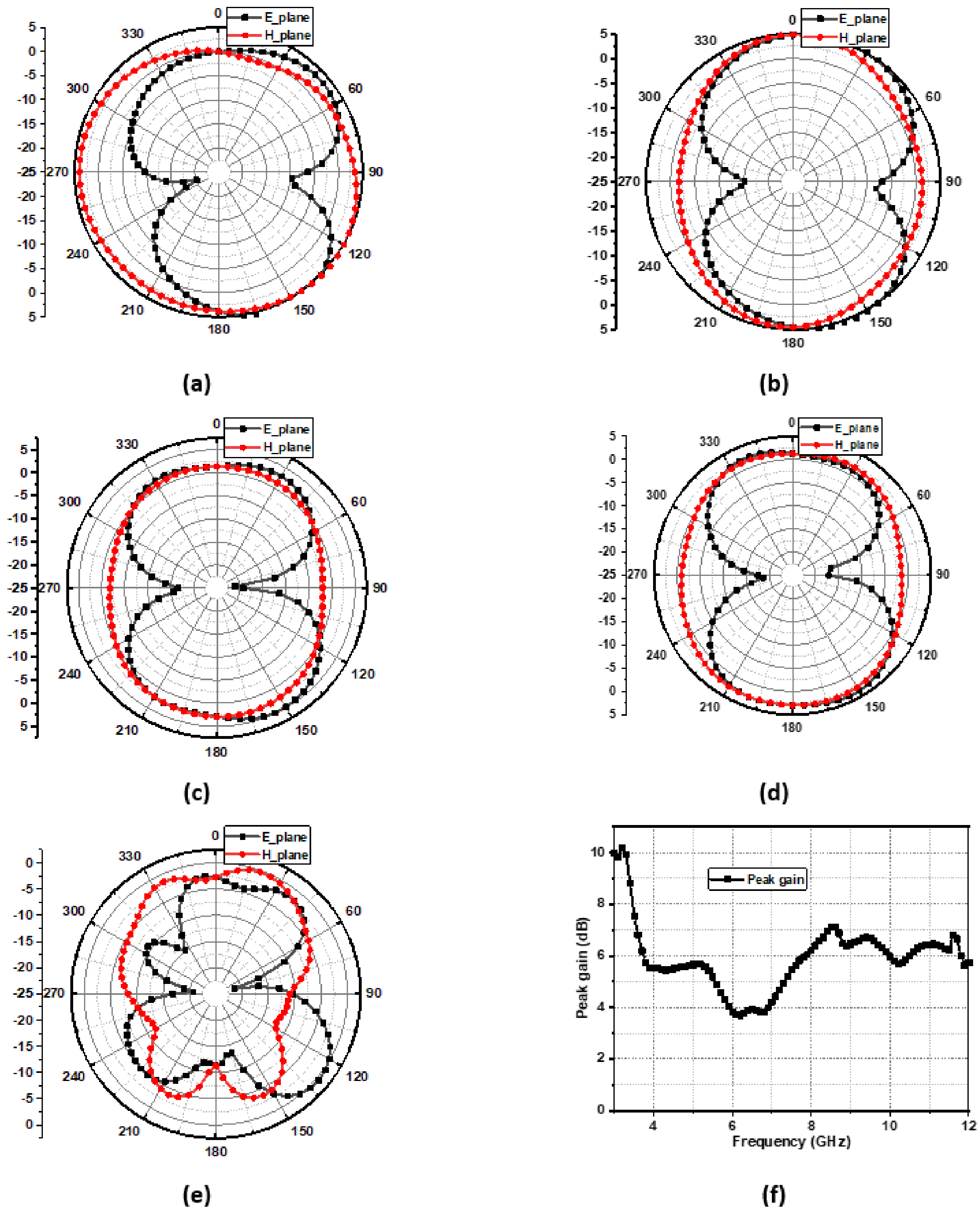

Figure 3

2–D radiation patterns of the UWB antenna at**a**3.4 GHz,**b**4 GHz,**c**5.6 GHz,**d**6 GHz,**e** 10 GHz**,** and **f** peak gain

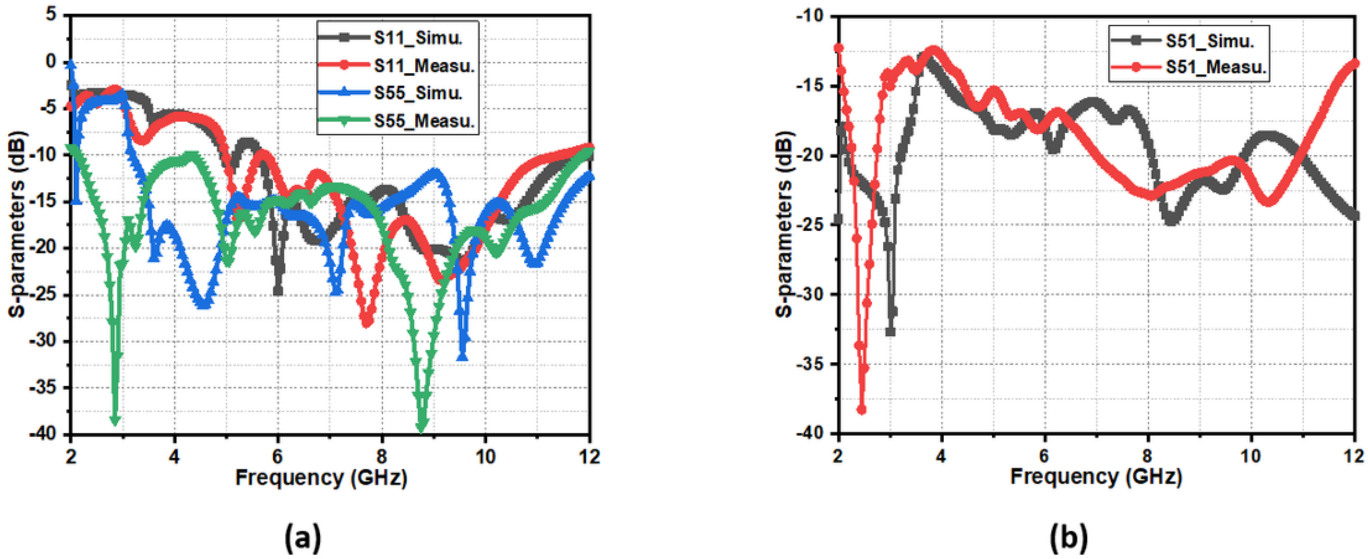

Figure 4

The Ant (P1) and the UWB antenna **a** Reflection, **b** Transmission coefficients

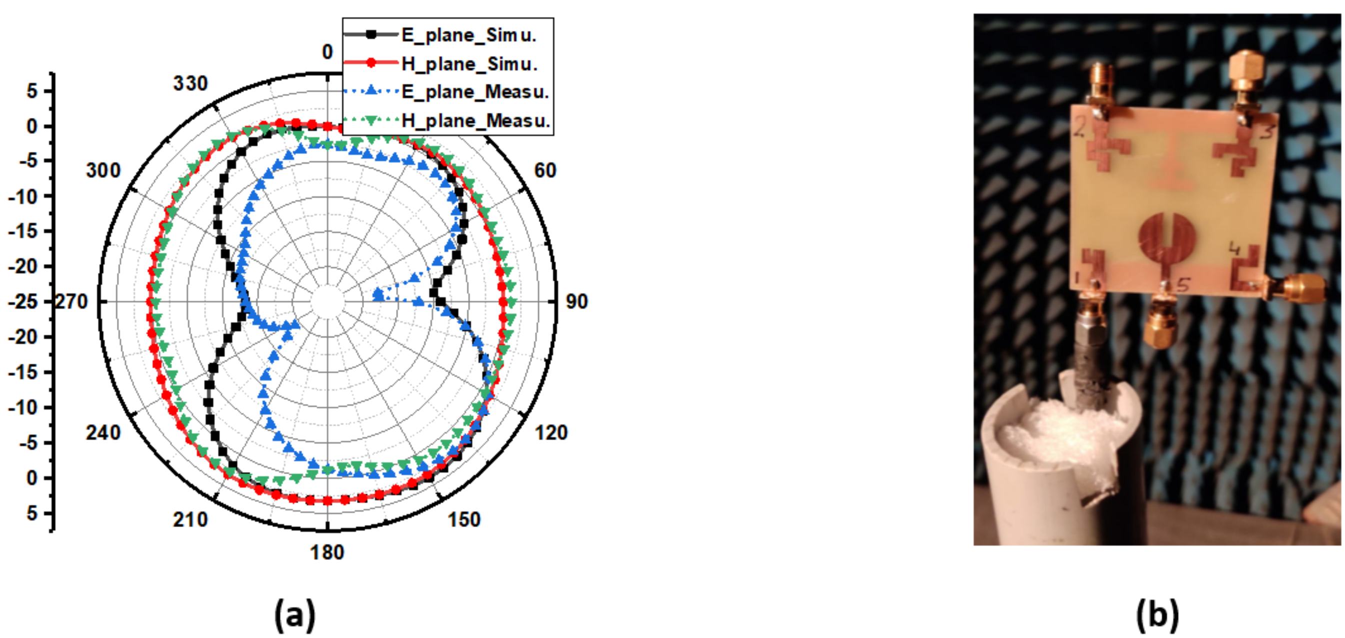

Figure 5

The Ant (P1) **a** Radiation pattern at 6 GHz, **b** Measurement setup

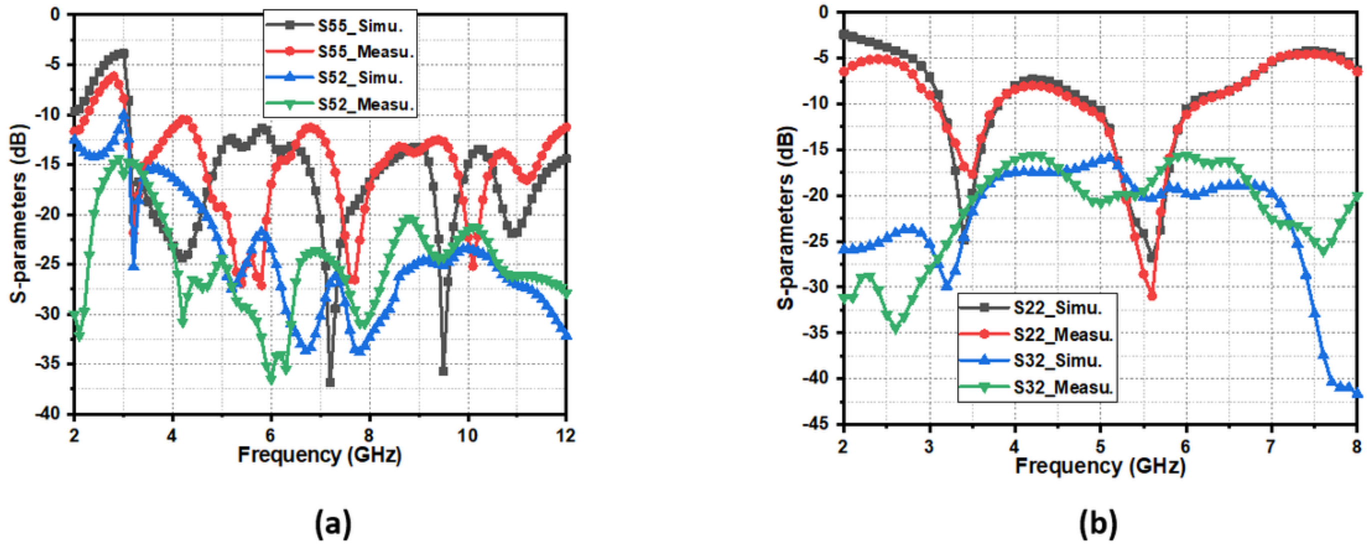

Figure 6

The UWB antenna, Ant (P2) and Ant (P3) S-parameters

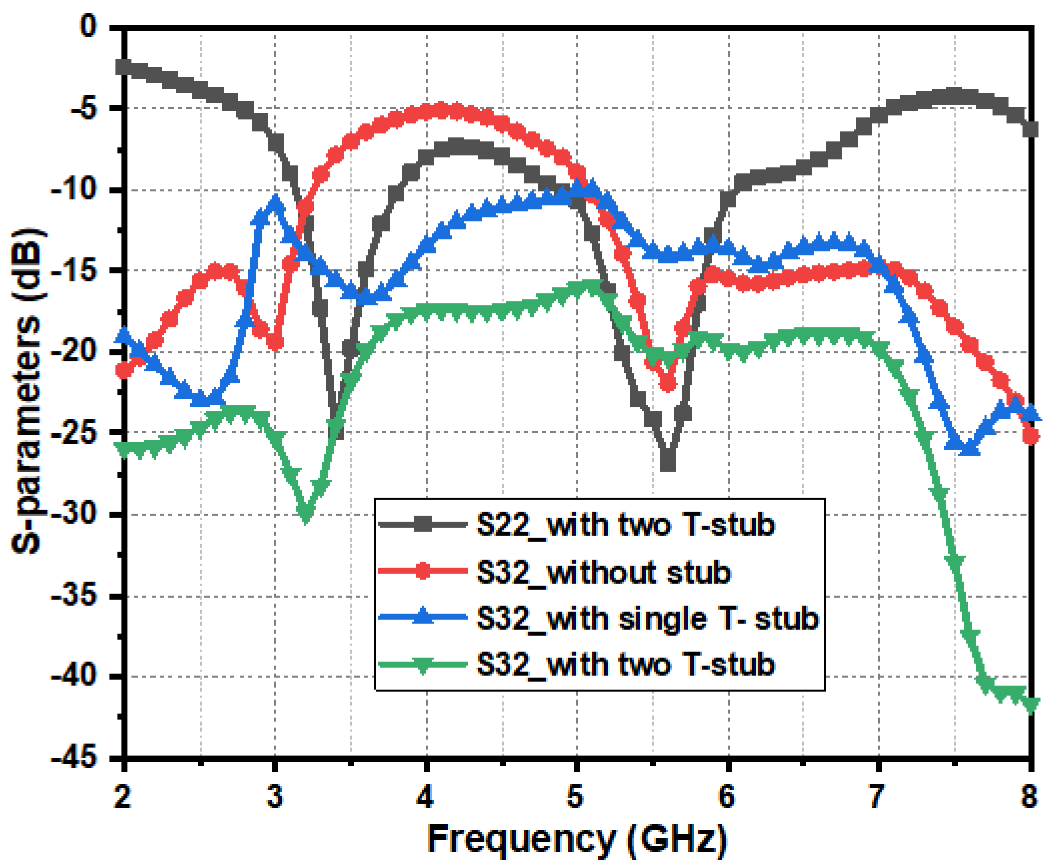

Figure 7

The simulated transmission coefficients between the P2 and P3 antenna elements with/without decoupling stub

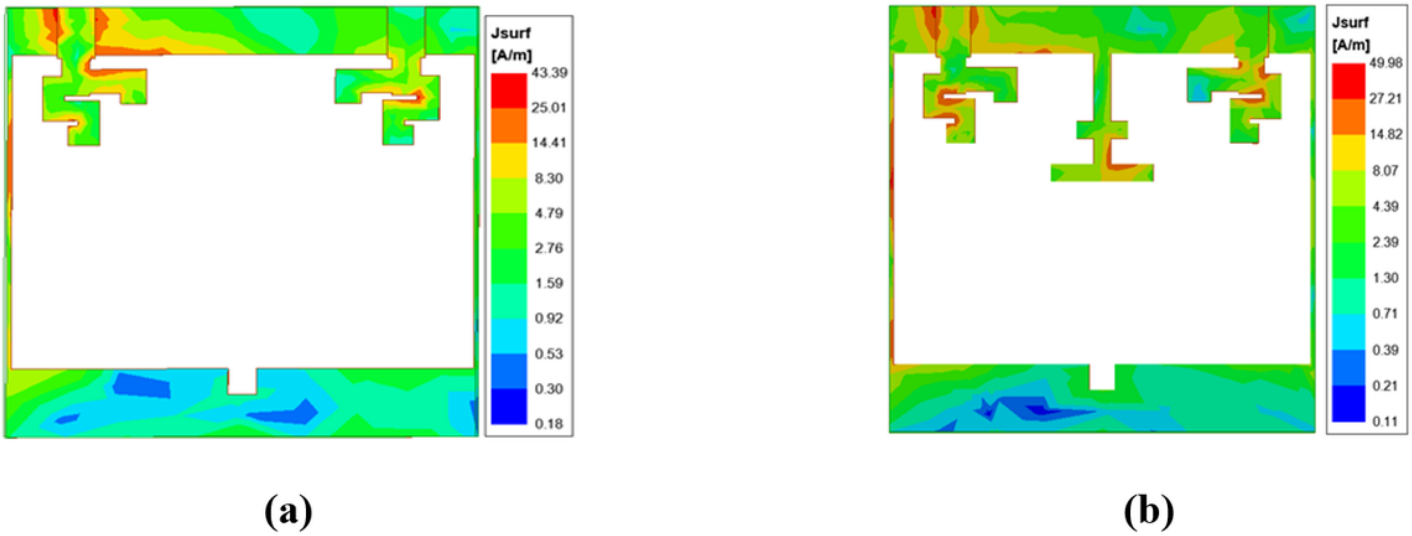

Figure 8

The surface current distribution **a** without, **b** with ground plane stub

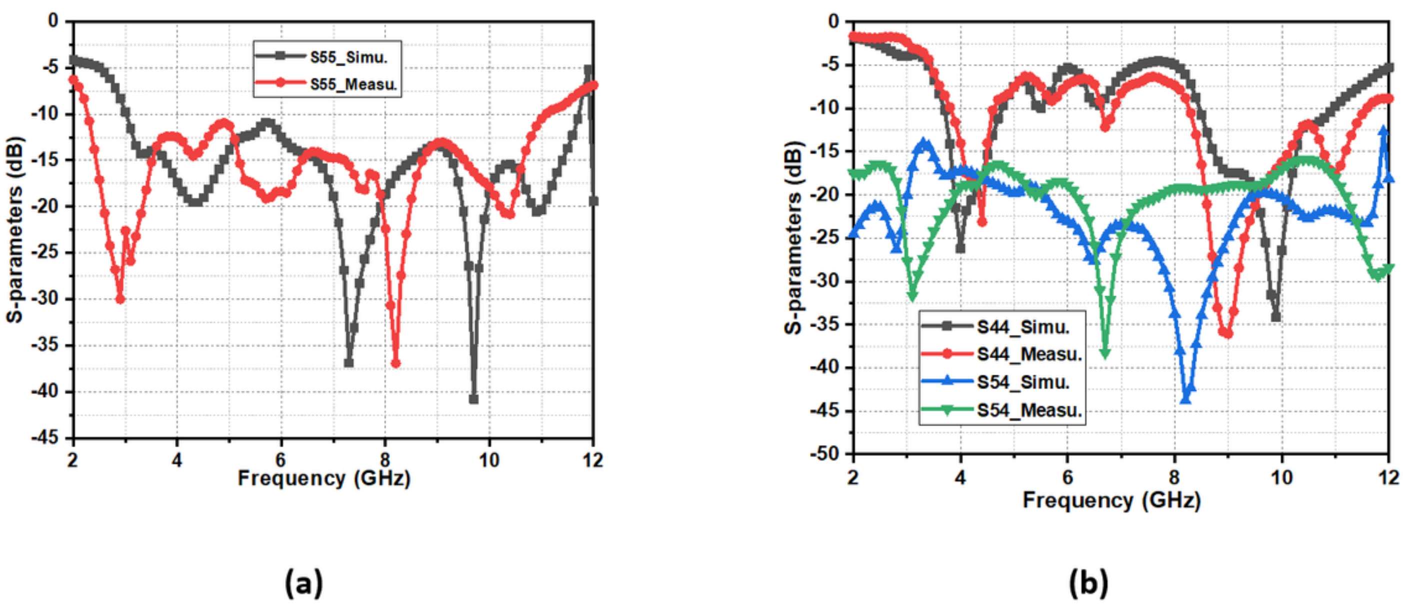

Figure 9

The simulated and measured S-parameters of the **a** UWB antenna, **b** Ant (P4)

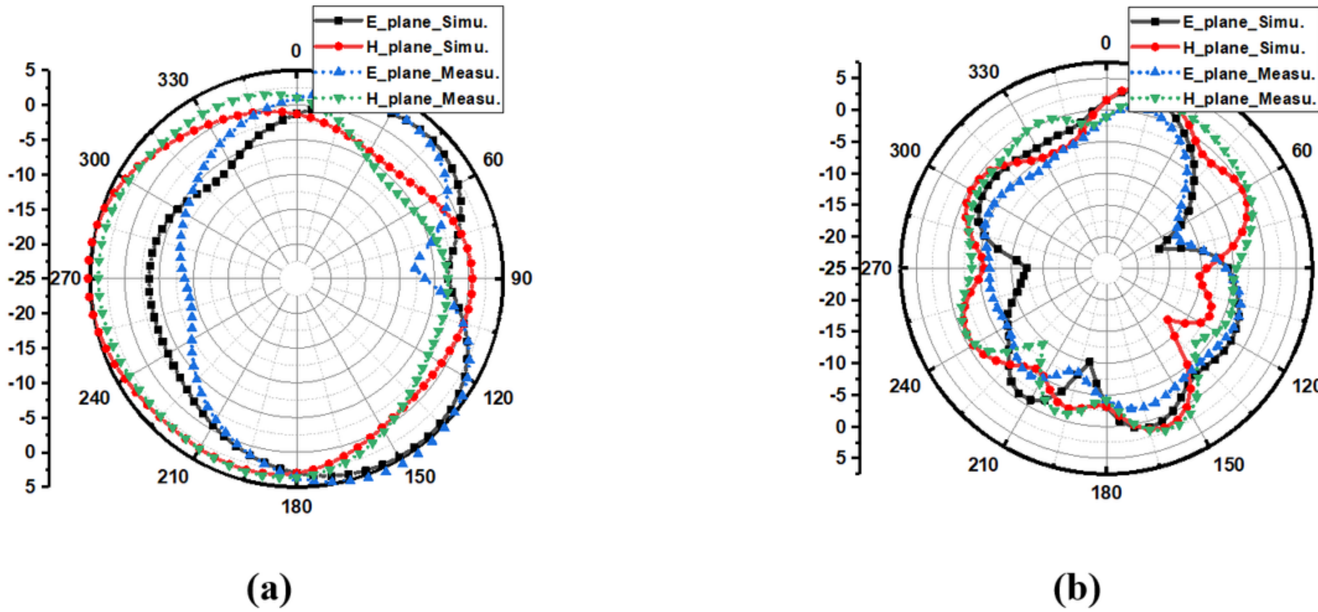

Figure 10

The radiation pattern of Ant (P4) at **a**4 GHz, **b** 10 GHz

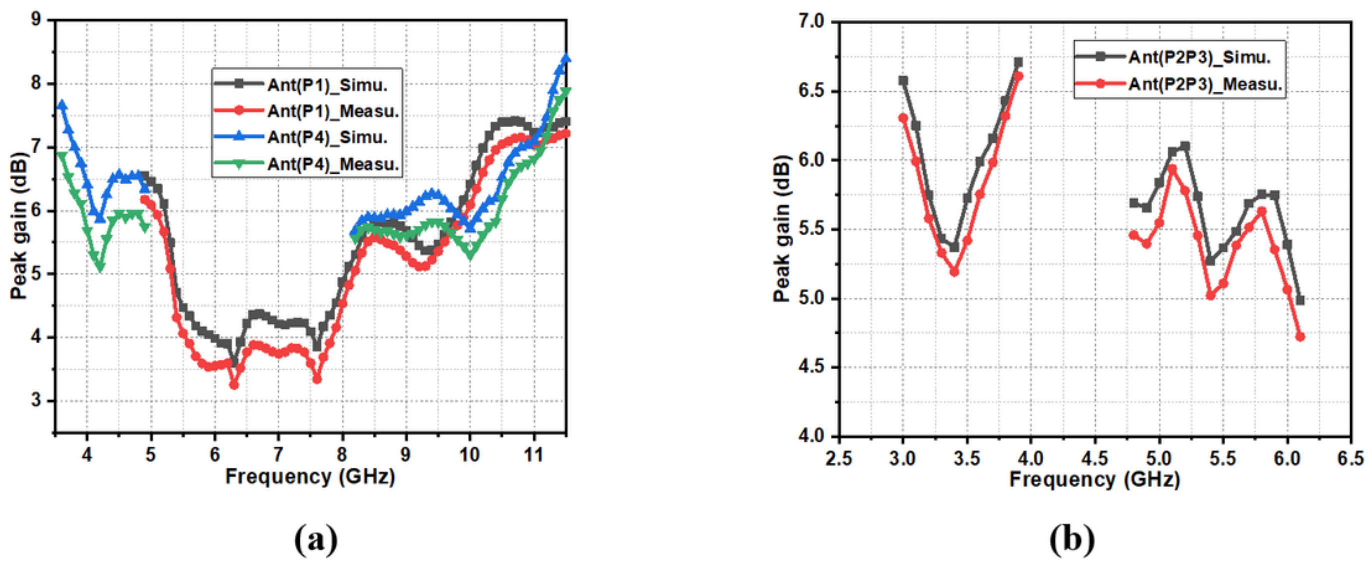

Figure 11

a Simulated, **b** Measured gain of the proposed antenna

(a) (b)

Figure 12

The fabricated antenna **a** Top view,**b** Bottom view

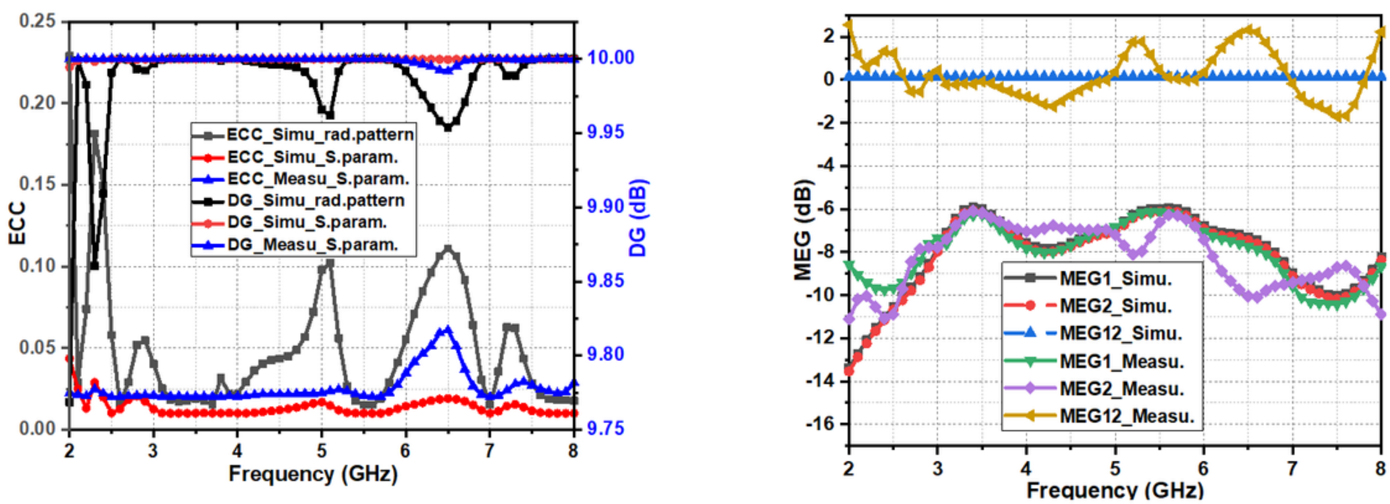

(a) (b)

Figure 13

The proposed MIMO antenna**a**ECC & DG, **b** MEG